

# Stiffness in stochastic chemically reacting systems: The implicit tau-leaping method

Muruhan Rathinam<sup>a)</sup>

*Department of Mathematics and Statistics, University of Maryland, Baltimore County, Baltimore, Maryland 21250*

Linda R. Petzold<sup>b)</sup>

*Computational Science and Engineering, University of California—Santa Barbara, Santa Barbara, California*

Yang Cao<sup>c)</sup>

*Computational Science and Engineering, University of California—Santa Barbara, Santa Barbara, California*

Daniel T. Gillespie<sup>d)</sup>

*Daniel T. Gillespie Consulting, Castaic, California*

(Received 13 January 2003; accepted 25 September 2003)

We show how stiffness manifests itself in the simulation of chemical reactions at both the continuous-deterministic level and the discrete-stochastic level. Existing discrete stochastic simulation methods, such as the stochastic simulation algorithm and the (explicit) tau-leaping method, are both exceedingly slow for such systems. We propose an implicit tau-leaping method that can take much larger time steps for many of these problems. © 2003 American Institute of Physics. [DOI: 10.1063/1.1627296]

## I. INTRODUCTION

In microscopic systems formed by living cells, the small numbers of reactant molecules can result in dynamical behavior that is discrete and stochastic rather than continuous and deterministic.<sup>1–4</sup> An analysis tool that respects these dynamical characteristics is the stochastic simulation algorithm (SSA), a numerical simulation procedure that is essentially exact for chemical systems that are spatially homogeneous or well stirred. Despite recent improvements,<sup>5</sup> as a procedure that simulates *every* reaction event, the SSA is necessarily inefficient for most realistic problems. There are two main reasons for this, both arising from the multiscale nature of the underlying problem: (1) *stiffness*, i.e., the presence of multiple time scales, the fastest of which are stable; and (2) the need to include in the simulation both species that are present in relatively small quantities and should be modeled by a discrete stochastic process, and species that are present in larger quantities and are more efficiently modeled by a deterministic differential equation (or at some scale in between). We emphasize that most chemical systems, whether considered at a scale appropriate to stochastic or to deterministic simulation, involve several widely varying time scales, so such systems are *nearly always stiff*.

In this paper we will address the problem of stiffness for discrete stochastic systems. We will demonstrate how stiffness is manifested in stochastic chemical kinetics, and show how to modify the recently proposed tau-leaping method<sup>6</sup> so

that much longer time steps can be taken for stiff systems.

The SSA, the tau-leaping method,<sup>6</sup> the modified tau-leaping method that will be introduced here, and deterministic ordinary differential equation (ODE) simulation are each most effective in certain situations. When the populations of all reactant species are small, the SSA will be as fast and efficient as one could reasonably wish. The goal of tau leaping was to speed up the SSA when either all reactant species are present in moderately large numbers, or (much more commonly) when some reactant species are present in small or moderate numbers while others are present in very large numbers. In such situations, significant stochastic effects can still arise, but tracking them with the SSA will be very time consuming. These situations can be expected to arise in many cellular systems of interest to biochemists. For those systems, the exact SSA is usually much too slow, while the deterministic reaction rate equation (RRE), though fast, fails to capture the stochastic effects. It was shown in Ref. 6 that tau leaping morphs into the SSA when all the molecular populations are very small, and morphs into the explicit Euler method for the RRE when all the molecular populations are very large. Our present work is aimed at formulating tau-leaping strategies that accurately and efficiently handle systems “in between” those two extremes.

The outline of this paper is as follows: In Sec. II we review simulation algorithms for chemical kinetics for a wide range of scales. In Sec. III we outline the problem of stiffness for the simulation of chemical kinetics systems at both the continuous and stochastic scales. In Sec. IV we propose an *implicit tau-leaping method* that overcomes the step size limitations due to stiffness of the explicit tau-leaping method, and we outline its implementation. Finally,

<sup>a)</sup>Electronic mail: muruhan@math.umbc.edu

<sup>b)</sup>Electronic mail: petzold@engineering.ucsb.edu

<sup>c)</sup>Electronic mail: ycao@engineering.ucsb.edu

<sup>d)</sup>Electronic mail: gillespiedt@mailaps.org

in Sec. V we present some numerical experiments demonstrating both the effectiveness and some limitations of the new implicit tau-leaping method.

## II. SIMULATION ALGORITHMS FOR CHEMICAL KINETICS

In a chemically reacting system involving  $N$  molecular species  $\{S_1, \dots, S_N\}$ , the state vector  $\mathbf{X}(t) \equiv (X_1(t), \dots, X_N(t))$ , where  $X_i(t)$  is the number of molecules of species  $S_i$  in the system at time  $t$ , will evolve stochastically because of the inherent randomness of thermal molecular motion. Stochastic molecular collisions give rise to stochastic chemical transmutations in accordance with a given set of  $M$  reaction channels  $\{R_1, \dots, R_M\}$ . If the system is well stirred and in thermal equilibrium, the dynamics of reaction channel  $R_j$  will be completely characterized by a propensity function  $a_j$  and a state-change vector  $\mathbf{v}_j = (v_{1j}, \dots, v_{Nj})$ :  $a_j(\mathbf{x})dt$  gives the probability that one  $R_j$  reaction will occur in state  $\mathbf{x}$  during the next infinitesimal time interval  $dt$ , and  $v_{ij}$  gives the change in the  $S_i$  molecular population induced by one  $R_j$  reaction.<sup>7</sup>

By appealing to the laws of probability theory, one can derive a chemical master equation (CME) that governs the time evolution of the probability density function of  $\mathbf{X}(t)$ , as well as a SSA that can generate numerical realizations of  $\mathbf{X}(t)$ . Both the CME and the SSA are exact consequences of the foregoing dynamical assumptions, so in spite of the difference in their descriptive thrusts, they are logically equivalent to each other.

The SSA simulates each successive reaction event that occurs in the system. It is a Monte Carlo method which proceeds from the fact that, if  $\mathbf{X}(t) = \mathbf{x}$ , then with

$$a_0(\mathbf{x}) \triangleq \sum_{j=1}^M a_j(\mathbf{x}),$$

the time  $\tau$  to the next reaction event is an exponentially distributed random variable with mean  $1/a_0(\mathbf{x})$ , and the index  $j$  of that next reaction is an integer random variable with probability  $a_j(\mathbf{x})/a_0(\mathbf{x})$ . Because the SSA simulates one reaction at a time, it will be very slow in the commonly occurring case that some reactions take place on a very fast time scale. Although exact methods have been proposed<sup>5</sup> that speed up the SSA, by itself it remains much too slow for practical simulation of realistic biological systems.

An *approximate* scheme called *tau leaping* has recently been proposed<sup>6</sup> to accelerate the SSA. The basic idea of tau leaping is as follows. Given a *preselected* time step  $\tau$  that encompasses more than one reaction event, if we could determine how many times each reaction channel fired during that time step, we might be able to forego knowing the precise instants at which those firings took place. In such a circumstance, we could leap along the system's history axis from one  $\tau$  subinterval to the next, instead of stepping along from one reaction event to the next. It has been shown<sup>6</sup> that this can be done *approximately* if  $\tau$  is taken small enough that the propensity functions remain nearly constant during the time step. The tau-leaping simulation method is an attempt to speed up the SSA by sacrificing some exactness. But, the approximate method must be used with circumspection, since while we are glad to leap over "unimportant" reaction events, we must take care not to leap over "important" ones.

To render these ideas more precisely, in tau leaping attention is focused on the set of  $M$  random variables

$$K_j(\tau; \mathbf{x}, t) \equiv \text{the number of times reaction channel } R_j \text{ fires in } [t, t + \tau), \text{ given that } \mathbf{X}(t) = \mathbf{x} \quad (j = 1, \dots, M). \quad (1)$$

It follows from the above definitions that if the system is in state  $\mathbf{x}$  and reaction  $R_1$  fires  $k_1$  times, and reaction  $R_2$  fires  $k_2$  times, etc., then the system will change to state  $\mathbf{x} + \sum_{j=1}^M k_j \mathbf{v}_j$ . Therefore, the random variables  $K_j(\tau; \mathbf{x}, t)$  defined in (1) completely determine the evolution of the system as follows: If  $\mathbf{X}(t) = \mathbf{x}$ , then for any  $\tau > 0$

$$\mathbf{X}(t + \tau) = \mathbf{x} + \sum_{j=1}^M K_j(\tau; \mathbf{x}, t) \mathbf{v}_j. \quad (2)$$

The simple (explicit) tau-leaping method makes the approximation

$$K_j(\tau; \mathbf{x}, t) \approx \mathcal{P}_j(a_j(\mathbf{x}), \tau),$$

where the  $\mathcal{P}_j$  are statistically independent Poisson random variables.<sup>8</sup> This approximation will be justified if  $\tau > 0$  is small enough that none of the propensity function values changes significantly during  $[t, t + \tau)$ . Thus, by (2), the explicit tau-leaping algorithm takes the following form: If  $\mathbf{X}(t) = \mathbf{x}$ , then for any such  $\tau$

$$\mathbf{X}(t + \tau) \approx \mathbf{x} + \sum_{j=1}^M \mathbf{v}_j \mathcal{P}_j(a_j(\mathbf{x}), \tau). \quad (3)$$

It has been shown<sup>6</sup> that this tau-leaping method is limited to the SSA method as the time step  $\tau$  becomes smaller than the mean time to the next reaction. In a forthcoming paper, we will present an analysis of this tau-leaping method, which in particular shows that the method is first-order accurate in  $\tau$ .

At the next coarser scale, suppose conditions are such that, starting in state  $\mathbf{x}$  at time  $t$  we can leap over an interval  $\tau$  that spans a *very large* number of firings of *every* reaction channel, yet all those firings induce only minuscule changes in the values of all the propensity functions. Then, since the Poisson random variable  $\mathcal{P}(a, t)$  will, when  $at \gg 1$ , be well approximated by the *normal* random variable  $\mathcal{N}(at, at)$ ,<sup>9</sup> the number of firings of channel  $R_j$  in  $[t, t + \tau)$  can be approximated by

$$K_j(\tau; \mathbf{x}, t) \approx \mathcal{P}_j(a_j(\mathbf{x}), \tau) \approx \mathcal{N}_j(a_j(\mathbf{x})\tau, a_j(\mathbf{x})\tau),$$

$$K_j(\tau; \mathbf{x}, t) \approx a_j(\mathbf{x})\tau + (a_j(\mathbf{x})\tau)^{1/2} \mathcal{N}_j(0, 1).$$

Substituting this into Eq. (2) yields the *Langevin method*: If  $\mathbf{X}(t) = \mathbf{x}$ , then for any  $\tau > 0$  that is small enough that none of the propensity function values changes significantly during  $[t, t + \tau)$ , but large enough that every reaction channel fires many more times than one

$$\mathbf{X}(t + \tau) \approx \mathbf{x} + \tau \sum_{j=1}^M \nu_j a_j(\mathbf{x}) + \tau^{1/2} \sum_{j=1}^M \nu_j a_j^{1/2}(\mathbf{x}) \mathcal{N}_j(0, 1), \quad (4)$$

where the  $\mathcal{N}_j(0, 1)$  are statistically independent normal random variables with means 0 and variances 1. Equation (4) is, in fact, the well-known first-order explicit method for simulating the *continuous* Markov process defined by the *chemical Langevin equation*.<sup>10,11</sup> A great deal of work in the past decade has gone into developing theory and numerical methods for equations of this type, which are known in the mathematical literature as stochastic differential equations (SDEs). Well-developed theory exists for determining the order of convergence of this and higher order methods for SDEs.<sup>12</sup> Some recent work has addressed automatic step size selection.<sup>13</sup>

Finally, in the limit of *infinitely* large molecular populations of all the reactant species, or more specifically in the *thermodynamic limit*, each term in the second summation on the right-hand side of Eq. (4) usually becomes vanishingly small compared to the correspondingly indexed term in the first summation.<sup>14</sup> Therefore, in that limit Eq. (4) usually reduces to, again with  $\mathbf{X}(t) = \mathbf{x}$

$$\mathbf{X}(t + \tau) \approx \mathbf{x} + \tau \sum_{j=1}^M \nu_j a_j(\mathbf{x}). \quad (5)$$

This will be recognized as the *explicit Euler method* for the numerical solution of the deterministic ODE system given by the *reaction rate equations* (which are more commonly scaled by the system volume).

### III. STIFFNESS

In *deterministic* systems of ODEs, stiffness generally manifests when there are well-separated “fast” and “slow” time scales present, and the “fast modes” are stable. Because of the fast stable modes, all initial conditions result in trajectories which, after a short and rapid transient, lead to the “stable manifold” where the “slow modes” determine the dynamics and the fast modes have decayed.

In general, a given trajectory of such a system will exhibit rapid change for a short duration (corresponding to the fast time scales) called the “transient,” and then evolve slowly (corresponding to the slow time scales). During the initial transient the problem is said to be nonstiff, whereas while the solution is evolving slowly it is said to be stiff. One would expect that a reasonable numerical scheme should be able to take larger time steps once the trajectory has come sufficiently close to the slow manifold without compromising the accuracy of the computed trajectory. That this is not always the case is well known to numerical analysts, and in general explicit methods are only able to perform well if they continue to take time steps that are of the order of the fastest time scale. This happens because explicit methods advance

the solution from one time to the next by approximating the slope of the solution curve at or near the beginning of the time interval. Since any numerical method makes errors on every time step, the numerical solution is never exactly on the stable manifold. Instead, it will be on some trajectory that approaches the stable manifold very rapidly. Thus, the approximation to the slope employed by explicit methods will always be on the order of the fastest time scale of the system. The very large slope decreases to almost zero in a time interval of the order of the fastest time scale. If the explicit numerical scheme continues to take small time steps of the order of these fast trajectories, then there is no problem. However, if the explicit method takes a larger time step, which would seemingly be appropriate for following the trajectories on the slow manifold, then the large estimated slope and the large time step lead to a point on the other side of the slow manifold, which is likely to be further away from it than was the previous point. This point is likely to have an even larger slope, leading to highly unstable oscillations.

An implicit method, on the other hand, does not approximate the slope of the trajectory near the beginning of the interval of a time step. Instead, it gives more weight to the slope at the unknown point at the end of the time step. This tends to avoid the above-described instability, but at the expense of having to solve a nonlinear system of equations for the unknown point at each time step. In fact, implicit methods often damp the perturbations off the slow manifold. Once the solution has reached the stable manifold, this damping keeps the solution on the manifold, and is desirable. Further details on stiffness in deterministic ODE systems can be found in Ref. 15 and the references therein.

The aim of this paper is to explore the nature of stiffness in discrete stochastic systems, to propose an implicit version of the (explicit) tau-leaping method discussed in Sec. II, and to demonstrate the extent to which the implicit method is effective for stiff, discrete stochastic systems.

When stochasticity is introduced into a system with fast and slow time scales, with fast modes being stable as before, one may still expect a slow manifold corresponding to the equilibrium of the fast scales. However, the picture changes in a fundamental way. After an initial rapid transient, while the mean trajectory is almost on the slow manifold, *any sample trajectory will still be oscillating at the fast time scale in a direction transverse to the slow manifold*. In some cases the size of the fluctuations off the slow manifold will be practically negligible. In those circumstances, an implicit scheme may take large steps, corresponding to the time scale of the slow mode. However, in other cases, the fluctuations off the slow manifold will *not* be negligible in size. In those instances, an implicit scheme that takes time steps much larger than the time scale of the fast dynamics will dampen these fluctuations, and will consequently fail to capture the variance correctly.

We will demonstrate that the implicit tau-leaping method can take large time steps for stiff, discrete stochastic systems, producing a solution which is accurate for the slow variables of the system, and for which the mean of the fast variables on the slow manifold is accurate. We will also show how the

distribution of the fast variables on the slow manifold can be recovered at relatively low cost.

#### IV. THE IMPLICIT TAU-LEAPING METHOD

The tau-leaping method described by Eq. (3) is an explicit method because the propensity functions  $a_j$  are evaluated at the current known state, so the future unknown random state  $\mathbf{X}(t + \tau)$  is given as an explicit function of  $\mathbf{X}(t)$ . Throughout the rest of the paper we shall refer to Eq. (3) as the *explicit-tau* method, and write it

$$\mathbf{X}^{(\text{et})}(t + \tau) = \mathbf{X}^{(\text{et})}(t) + \sum_{j=1}^M \mathbf{v}_j \mathcal{P}_j(a_j(\mathbf{X}^{(\text{et})}(t)), \tau), \quad (6)$$

where the superfix “et” stands for explicit tau. We mentioned in Sec. III that the explicit Euler method exhibits instability for stiff systems with large step sizes. The explicit-tau method is essentially an extension of the explicit Euler method to discrete stochastic systems, and as such it too has poor stability. In this section we motivate and derive an implicit tau-leaping method. In Sec. V we will present numerical experiments that demonstrate the accuracy and efficiency of this method, as compared to the explicit-tau method and the SSA.

To motivate our formulation of the implicit-tau method, we look again at the explicit-tau method (6). Here, the increment in the state  $\mathbf{X}^{(\text{et})}(t + \tau) - \mathbf{X}^{(\text{et})}(t)$  is given by a linear combination of statistically independent Poisson random variables  $\mathcal{P}_j(a_j, \tau)$ , whose parameters  $a_j$  are evaluated at  $\mathbf{X}^{(\text{et})}(t)$ . An attempt to completely implicitize the method would require generating Poisson random variables  $\mathcal{P}_j(a_j, \tau)$ , with the  $a_j$  evaluated at the unknown random state  $\mathbf{X}(t + \tau)$  that we are trying to find. Since it is not entirely clear how to interpret and solve such an equation, we will attempt a partial implicitization. To this end, let us regard each of the random variables  $\mathcal{P}_j$  as the sum of two parts, one being the mean value  $a_j \tau$  of  $\mathcal{P}_j$ , and the other being the zero-mean random variable  $\mathcal{P}_j - a_j \tau$ . We then evaluate the mean value part  $a_j \tau$  at the unknown state  $\mathbf{X}(t + \tau)$ , and the zero-mean random part  $\mathcal{P}_j - a_j \tau$  at the known state  $\mathbf{X}(t)$ . Thus, we arrive at an implicit method described by

$$\begin{aligned} \mathbf{X}^{(\text{it})}(t + \tau) = & \mathbf{X}^{(\text{it})}(t) + \sum_{j=1}^M \mathbf{v}_j a_j(\mathbf{X}^{(\text{it})}(t + \tau)) \tau \\ & + \sum_{j=1}^M \mathbf{v}_j (\mathcal{P}_j(a_j(\mathbf{X}^{(\text{it})}(t)), \tau) - a_j(\mathbf{X}^{(\text{it})}(t)) \tau). \end{aligned} \quad (7)$$

Here, the random variables  $\mathcal{P}_j$  are, as before, statistically independent Poisson random variables. In a forthcoming paper, we will present an analysis of the accuracy and stability properties of this method, which in particular shows that the method is accurate to first order in  $\tau$ .

We note that in the implementation of the method (7), the random variables  $\mathcal{P}_j(a_j(\mathbf{X}^{(\text{it})}(t)), \tau)$  can be generated without knowing  $\mathbf{X}^{(\text{it})}(t + \tau)$ . Once the  $\mathcal{P}_j(a_j(\mathbf{X}^{(\text{it})}(t)), \tau)$  have been generated, the unknown state  $\mathbf{X}^{(\text{it})}(t + \tau)$  depends on  $\mathcal{P}_j(a_j(\mathbf{X}^{(\text{it})}(t)), \tau)$  in a deterministic way, even though

this dependence is given by an implicit equation. As is done in the case of deterministic ODE solution by implicit methods,  $\mathbf{X}^{(\text{it})}(t + \tau)$  can be computed by applying Newton's method for the solution of nonlinear systems of equations to (7) where the  $\mathcal{P}_j(a_j(\mathbf{X}^{(\text{it})}(t)), \tau)$  are all known values.

Just as the explicit-tau method segues to the explicit Euler methods for SDEs and ODEs, the implicit-tau method segues to the implicit Euler methods for SDEs and ODEs. In the SDE regime we get, approximating Poissons by normals

$$\begin{aligned} \mathbf{X}^{(\text{it})}(t + \tau) \approx & \mathbf{X}^{(\text{it})}(t) + \tau \sum_{j=1}^M \mathbf{v}_j a_j(\mathbf{X}^{(\text{it})}(t + \tau)) \\ & + \tau^{1/2} \sum_{j=1}^M \mathbf{v}_j a_j(\mathbf{X}^{(\text{it})}(t))^{1/2} \mathcal{N}_j(0, 1), \end{aligned} \quad (8)$$

where  $\mathcal{N}_j(0, 1)$  are independent normal random variables with mean zero and variance 1. This is precisely the implicit Euler version of (4).<sup>12</sup>

In the thermodynamic limit<sup>14</sup> where random terms in the above SDE system may be ignored, the implicit-tau method becomes the implicit Euler method

$$\mathbf{X}(t + \tau) = \mathbf{X}(t) + \tau \sum_{j=1}^M \mathbf{v}_j a_j(\mathbf{X}(t + \tau)), \quad (9)$$

for the corresponding deterministic reaction rate equations.

It is well known that, for stiff ODE systems, the implicit Euler method has a strong damping property. Indeed, it is this property that makes the implicit Euler method so desirable for such systems: Once the solution is close enough to the slow manifold that the step size can be increased, the method damps out any errors and keeps the solution close to the slow manifold. The implicit tau-leaping method inherits this damping property, which is still advantageous for taking large time steps and staying close to the slow manifold. However, as a consequence of this property, the method will also damp out the natural fluctuations of the fast variables. So, while the implicit tau-leaping method computes the *slow* variables with their correct distributions, it computes the *fast* variables with the correct means but with distributions about those means that are too narrow.

We have developed a time-stepping strategy that is intended to *restore* the overly damped fluctuations in the fast variables. The idea is to interlace the implicit tau leaps, each of which is on the order of the time scale of the slow variables and hence “large,” with a sequence of much smaller time steps, each of which is on the order of the time scale of the fast variables. The smaller time steps are to be taken over a duration that is comparable to the “relaxation/decorrelation” time of the fast variables. These small time steps may be executed using either the explicit-tau method or the implicit-tau method. This sequence of small steps is intended to “regenerate” the correct statistical distributions of the fast variables, which have been made too narrow by the preceding large implicit tau-leaps. The fact that the underlying kinetics is Markovian or “past-forgetting” is important in being able to apply such a procedure. The optimal interlacing

strategy and the choice of explicit versus implicit tau for the small time steps is the subject of further research.

In the next section, our first example will illustrate the damping of the fluctuations in the fast variables caused by successive large implicit-tau leaps, and then the successful regeneration of those fluctuations through a sequence of ten successive small implicit-tau leaps, all with a very substantial net gain in computational efficiency.

Finally, we note that the implicit-tau method (7) has the property that the state change  $\mathbf{X}^{(it)}(t+\tau) - \mathbf{X}^{(it)}(t)$  is generally not an integer vector. It is possible to avoid noninteger state changes by modifying the implicit-tau method. It might be tempting to do this by simply rounding every component of  $\mathbf{X}^{(it)}(t+\tau)$  to the nearest integer. But, it is better to ensure that the state change be *stoichiometrically realizable*; i.e., not only should the state change be an integer vector, but it should also be a sum of the form  $k_1 \mathbf{v}_1 + \dots + k_M \mathbf{v}_M$ , where  $k_1, \dots, k_M$  are non-negative integers. This way, the state change can be interpreted as the result of reaction channel  $R_j$  firing  $k_j$  times for  $j=1, \dots, M$ . This yields the following implicit method: First, compute  $\mathbf{X}' = \mathbf{X}(t+\tau)$  according to (7), i.e., by using Newton's method to solve the implicit equation

$$\mathbf{X}' = \mathbf{x} + \sum_{j=1}^M \mathbf{v}_j a_j(\mathbf{X}') \tau + \sum_{j=1}^M \mathbf{v}_j (\mathcal{P}_j(a_j(\mathbf{x}), \tau) - a_j(\mathbf{x}) \tau), \quad (10)$$

where  $\mathbf{x}$  is the system's state at time  $t$ . Then, approximate the number of firings  $K_j(\tau; \mathbf{x}, t)$  of the reaction channel  $R_j$  in the time interval  $[t, t+\tau]$  by the *integer-valued* random variable  $\hat{K}_j(\tau; \mathbf{x}, t)$ , defined by

$$\hat{K}_j(\tau; \mathbf{x}, t) = [a_j(\mathbf{X}') \tau + \mathcal{P}_j(a_j(\mathbf{x}), \tau) - a_j(\mathbf{x}) \tau]. \quad (11)$$

Here, the  $\mathcal{P}_j(a_j(\mathbf{x}), \tau)$  for  $j=1, \dots, M$  are the *same numbers* used in Eq. (10), and  $[z]$  denotes the nearest non-negative integer corresponding to a real number  $z$ . Finally, invoking (2), estimate the state at time  $t+\tau$  as

$$\mathbf{X}(t+\tau) = \mathbf{x} + \sum_{j=1}^M \mathbf{v}_j \hat{K}_j(\tau; \mathbf{x}, t). \quad (12)$$

Although this modification might be prudent for some systems, for the simple systems we have studied thus far the original version of the implicit-tau method has performed as well as this "rounded" version. Therefore, in the remainder of this paper we will focus on the original "unrounded" implicit-tau method.

## V. NUMERICAL EXPERIMENTS

### A. Example 1

This problem, the decaying-dimerizing reaction set studied in Ref. 6, consists of three species  $S_1$ ,  $S_2$ , and  $S_3$  and four reaction channels

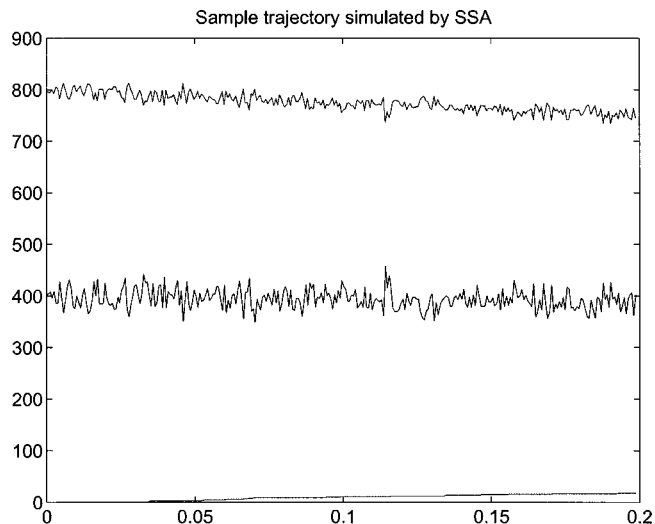
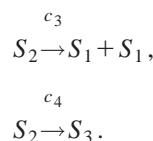


FIG. 1. Sample trajectories for example 1, simulated by the exact SSA. The upper curve is  $x_2$ , the middle curve is  $x_1$ , and the lower curve is  $x_3$ .



We chose values for the parameters

$$c_1 = 1, \quad c_2 = 10, \quad c_3 = 1000, \quad c_4 = 0.1,$$

which will render the problem stiff. The initial conditions  $x_1(0) = 400$ ,  $x_2(0) = 798$ , and  $x_3(0) = 0$  were chosen to lie on the approximate slow manifold given by the equation

$$x_2 = \frac{5}{1000} x_1 (x_1 - 1).$$

This avoids the inconvenience for the constant-step size algorithms under study of having to take small steps during the initial transient, and large steps on the slow manifold. The propensity functions are given by

$$a_1 = x_1, \quad a_2 = 5x_1(x_1 - 1), \quad a_3 = 1000x_2, \quad a_4 = 0.1x_2,$$

and the problem was solved on the time interval  $[0, 0.2]$ .

Figure 1 depicts sample trajectories as simulated by the exact SSA. Figure 2 shows the same sample trajectory of  $x_3$ , on a more revealing scale for that variable. We note that while  $x_1$  and  $x_2$  vary rapidly,  $x_3$  varies slowly. All three variables  $x_1$ ,  $x_2$ , and  $x_3$  exhibit random behavior,  $x_3$  being the most random. Figures 3, 4, and 5 show the histograms for the final state values, comparing SSA with explicit tau leaping. Each histogram was obtained by simulating an ensemble of 10 000 trajectories. The explicit tau leaping was performed with a constant step size of  $2 \times 10^{-5}$ .

It is evident from Figs. 3, 4, and 5 that the explicit-tau method captures the statistics of the final states very well, with only 10 000 time steps over the interval, whereas the SSA required on average 310 000 time steps. In terms of computation time, 10 000 simulations using SSA took 5697 CPU seconds, while 10 000 simulations using explicit tau

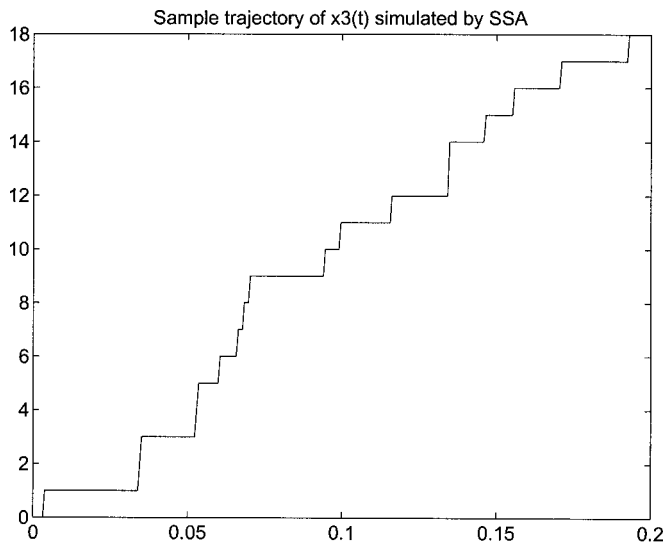


FIG. 2. Sample trajectory  $x_3(t)$  in example 1, simulated by SSA.

with a constant step size of  $2 \times 10^{-5}$  took 731 CPU seconds. These computations were performed on a 1.4 Ghz Pentium IV Linux workstation.

Figure 6 shows that the explicit-tau method becomes unstable at step sizes roughly equal to or larger than  $2.2 \times 10^{-4}$ . This is the stability limit that would be predicted by a linearized stability analysis of the forward Euler method applied to the corresponding deterministic ODE model. In a forthcoming paper, we will address stability criteria and analysis for discrete stochastic systems.

To verify that the implicit-tau method can take much larger time steps while maintaining accuracy, we simulated an ensemble of 10 000 trajectories using explicit tau with constant step size  $10^{-4}$  and implicit tau with constant step size 0.01. The step size  $10^{-4}$  for explicit tau was chosen to be as large as possible without compromising accuracy (it is near the stability limit of  $2.2 \times 10^{-4}$ ). Figures 7–9 compare the final state relative bin frequencies computed by all three

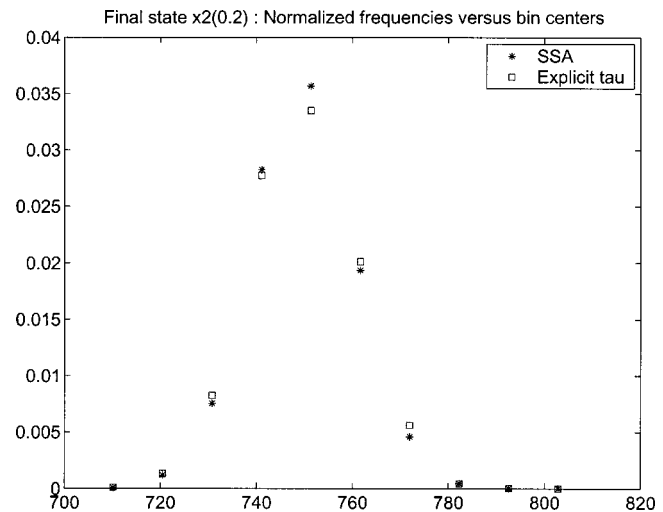


FIG. 4. Final state histogram for  $x_2$  in example 1, computed by the SSA (stars) and the explicit-tau method (squares), the latter with constant step size  $2 \times 10^{-5}$ .

methods. Tables I and II show the sample means and standard deviations for the final states estimated by the three methods. For the means, we also present the solution from the ODE solver in MATLAB. The results show that the ODE solver with automatic step sizing captures the mean quite accurately. However, neither the ODE model nor the solver gives us any indication of the nontrivial amount of fluctuation of the states about their mean values.

It is clear from the histograms that if the goal is to capture the slow state  $x_3$  including its randomness (which is significant), then implicit tau is far superior to explicit tau, because it achieves comparable accuracy with a factor of 100 fewer steps. Although the computational effort per step is greater for implicit tau than explicit tau, this is far outweighed by implicit tau's ability to take much larger steps. The computation time for 10 000 implicit-tau simulations

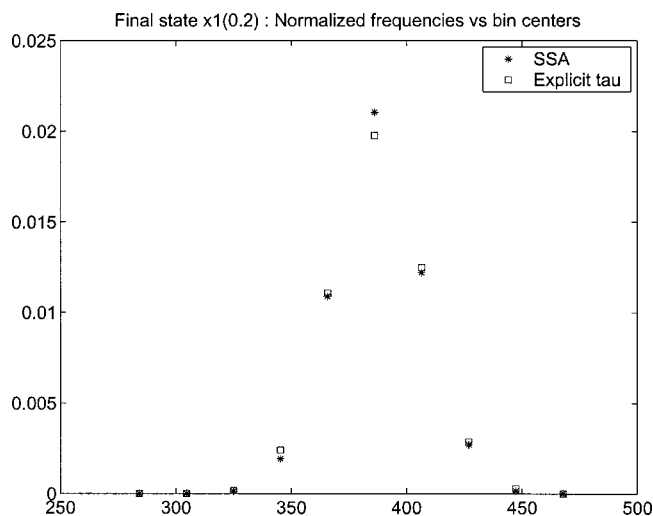


FIG. 3. Final state histogram for  $x_1$  in example 1, computed by the SSA (stars) and the explicit-tau method (squares), the latter with constant step size  $2 \times 10^{-5}$ .

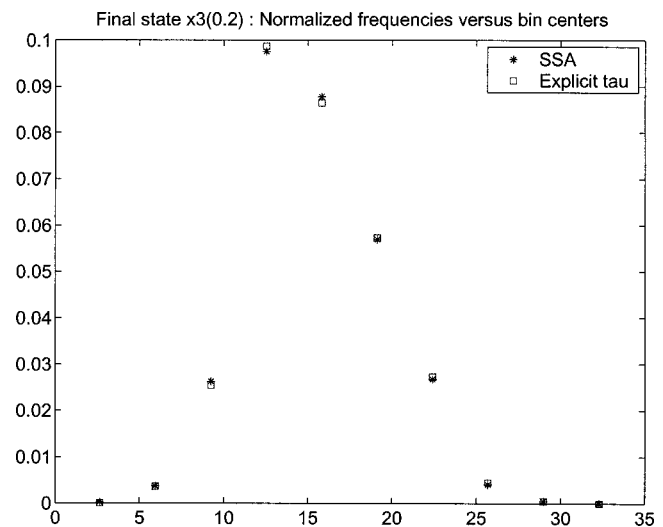


FIG. 5. Final state histogram for  $x_3$  in example 1, computed by the SSA (stars) and the explicit-tau method (squares), the latter with constant step size  $2 \times 10^{-5}$ .

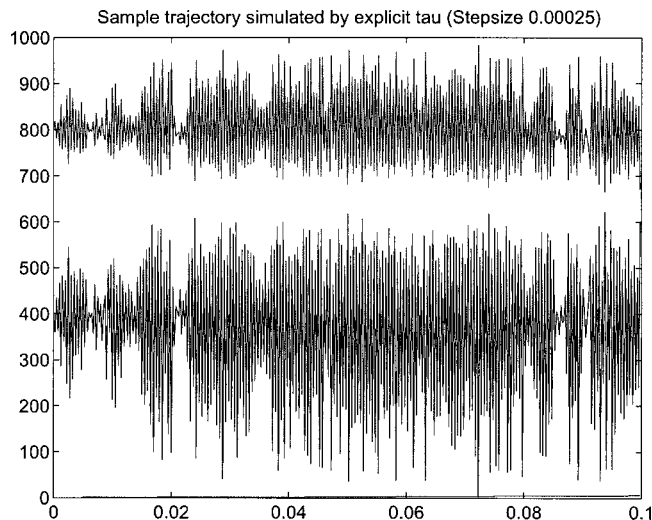


FIG. 6. Sample trajectories for example 1 as simulated by the explicit-tau method with step size  $2.5 \times 10^{-4}$ . The trajectories develop unstable oscillations, and yield unrealistic negative states beyond  $t \approx 0.1$ .

was 15 CPU seconds, as compared to 731 CPU seconds for explicit tau and 5697 CPU seconds for SSA.

On the other hand, if one is interested in capturing the fluctuations of the fast variables  $x_1$  and  $x_2$ , then implicit tau with these large time steps will not be adequate. In order to capture the distributions of  $x_1$  and  $x_2$ , we used the technique described in Sec. IV of interlacing small time steps with large time steps. In this example, we took the first 19 steps with implicit tau using step size 0.01 as before. Then, implicit tau was used to take one step of size 0.0098. For the remaining time of 0.002 we took ten steps of size  $2 \times 10^{-5}$  using implicit tau. The first 20 steps are the large steps which capture the *mean* values of all the state variables, and the noise in the slow variable, accurately. The last ten small steps recover the distribution information of the fast variables  $x_1$  and  $x_2$ . The time period to recover the distribution informa-

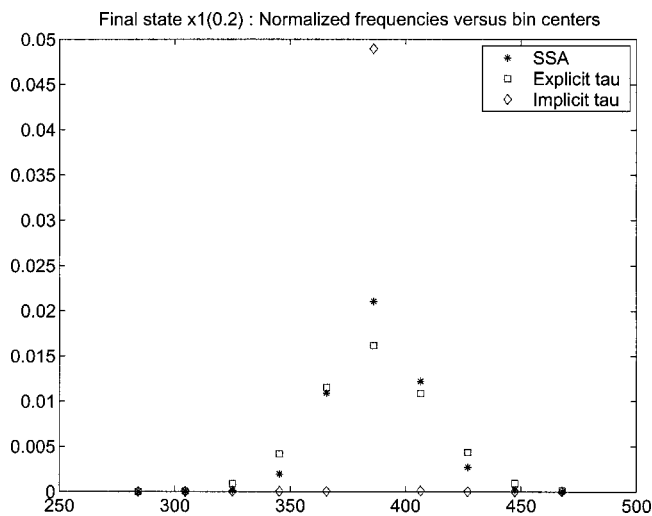


FIG. 7. Final state histogram for  $x_1$  in example 1, as computed by the SSA (stars), the explicit-tau method with step size  $1 \times 10^{-4}$  (squares) and the implicit-tau method with step size 0.01 (diamonds). Note that the explicit-tau method overestimates the noise while the implicit-tau method underestimates it.

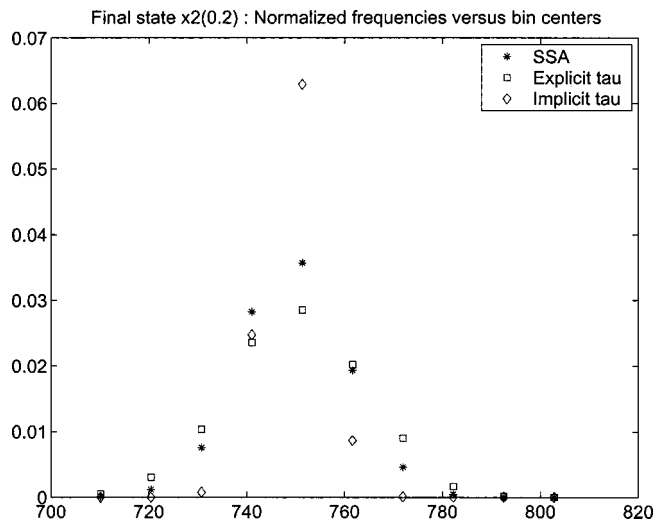


FIG. 8. Final state histogram for  $x_2$  in example 1, as computed by the SSA (stars), the explicit-tau method with step size  $1 \times 10^{-4}$  (squares), and the implicit-tau method with step size 0.01 (diamonds). Note that the explicit-tau method overestimates the noise while the implicit-tau method underestimates it.

tion is roughly the “relaxation time” of the fast variables. The final state histogram for this simulation is compared with that of the SSA in Figs. 10–12, and shows good agreement with SSA for all three variables  $x_1$ ,  $x_2$ , and  $x_3$ . The computation time for 10 000 simulations using this interlaced method was only 23 CPU seconds (much less compared with the 731 CPU seconds for the explicit-tau simulations in Figs. 3–5 and the 5697 CPU seconds for the SSA simulations of the same problem). Thus, the interlaced implicit tau is able to capture the statistics of all the state variables accurately with significant computational advantage over both SSA and explicit tau.

In this example, we were able to capture the distributions of all state variables at the final time with only one recovery

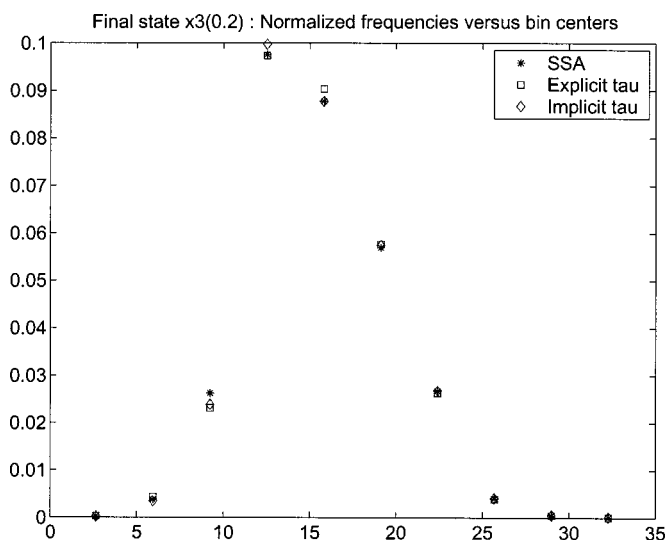


FIG. 9. Final state histogram for  $x_3$  in example 1, as computed by the SSA (stars), the explicit-tau method with step size  $1 \times 10^{-4}$  (squares), and the implicit-tau method with step size 0.01 (diamonds).

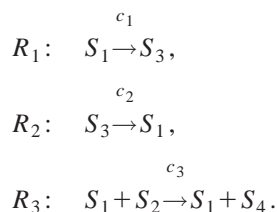
TABLE I. Sample means (for a sample size of  $n=10\,000$ ) for the final states in example 1 as computed by SSA, explicit-tau, the original implicit-tau, and the interlaced implicit-tau methods, with step sizes as described in the text. Also shown for comparison purposes are the predictions of the corresponding deterministic ODE.

	ODE	SSA	Explicit tau	Implicit tau	Interlaced implicit tau
Sample mean: $x_1(0.2)$	387.7	387.3	386.2	387.6	387.2
Sample mean: $x_2(0.2)$	749.3	749.5	750.1	749.5	749.4
Sample mean: $x_3(0.2)$	15.47	15.45	15.48	15.42	15.59

period. In general, it may be necessary to do the recovery steps more often. An optimal strategy for the interlacing procedure is a topic for further research.

## B. Example 2

In some stiff systems, the fast variables exhibit near-deterministic behavior while the slow variables still exhibit randomness. In such cases, implicit tau will clearly be the method of choice, as can be demonstrated using the simple reaction set



Since the total number of  $S_1$  and  $S_3$  molecules is constant (say  $x_T$ ), and if we don't care about the by-product  $S_4$ , we can model this system with two variables  $x=(x_1, x_2)$  (i.e., numbers of  $S_1$  and  $S_2$  molecules, respectively) and three reactions. The propensity functions are

$$\begin{aligned}
 a_1(x) &= c_1 x_1, \\
 a_2(x) &= c_2 (x_T - x_1), \\
 a_3(x) &= c_3 x_1 x_2.
 \end{aligned}$$

The stoichiometric vectors are  $\nu_1=(-1,0)^T$ ,  $\nu_2=(1,0)^T$ , and  $\nu_3=(0,-1)^T$ . We chose  $c_1=c_2=10^5$ ,  $c_3=0.0005$ , and  $x_T=20\,000$ , with initial condition  $x(0)=(10\,000,100)$ .

Since  $c_1=c_2$ , then  $x_1=x_T/2$  will be an equilibrium value for  $x_1$ . The dynamics of  $x_1$  is independent of  $x_2$ , but the dynamics of  $x_2$  depends on  $x_1$ . Also, note that the reactions  $R_1$  and  $R_2$  are much faster than  $R_3$ .

Since the dynamics of  $x_1$  alone is the same as in the simple reversible isomerization problem,<sup>11</sup> the exact asymptotic mean and variance can be computed analytically (see the Appendix). The equilibrium value  $x_1=10\,000$  is the asymptotic mean, and the asymptotic standard deviation of

$x_1$  is given by  $\sqrt{c_1 x_\infty / (c_1 + c_2)} = \sqrt{10\,000/2} = 70.7$  (here,  $x_\infty$  is the asymptotic mean value, which in our case is  $x_T/2$ ). This is less than 1% of the equilibrium value. Thus, we may regard the noise in  $x_1$  as negligible. But, as we shall see, the noise in  $x_2$  cannot be regarded as negligible.

We simulated an ensemble of 10 000 trajectories using all three methods: SSA, explicit tau with constant step size  $5 \times 10^{-6}$  (half the size of the maximum value to maintain stability), and implicit tau with constant step size 0.005, all to estimate the final state at time  $T=0.01$ .

Table III shows the sample means and standard deviations for the final state of  $x_2$  estimated by the three methods. For the means, we also show the solution from the ODE solver in MATLAB. Figures 13 and 14 compare the final state histograms computed by explicit tau and implicit tau with those computed by SSA. The full behavior of the noisy variable  $x_2$  is adequately reproduced by both tau-leaping methods, while the inaccuracies of both methods in the estimations of the fluctuations in  $x_1$  are inconsequential because of their smallness. The implicit-tau method is superior to the explicit-tau method, since the former takes two steps for each trajectory while the latter takes 2000. The explicit-tau method in turn is superior to the SSA, which takes on average  $2 \times 10^7$  time steps for each trajectory.

Note that in this reaction, one can make the relative size of the equilibrium noise in  $x_1$  arbitrarily small by scaling up  $c_1$  and  $c_2$  and  $x_1(0)=x_T/2$  by the same factor. This leaves the stiffness ratio  $[2(c_1+c_2)]/c_3 x_T$  unchanged but makes the noise in  $x_1$  as small as we want compared to its equilibrium value. For instance, if we choose  $c_1=c_2=10^6$  and  $x(0)=(10^6,100)$  then the equilibrium noise of  $x_1$  will have a standard deviation of  $\sqrt{50\,000} \approx 224$ , which is 0.02% of the equilibrium value  $10^6$ . Thus, the noise will be less than what we obtained with our choice for  $c_1$ ,  $c_2$ , and  $x_T$ . We did not choose the values  $c_1=c_2=10^6$  and  $x_T=200\,000$  because the SSA simulation takes an extremely long time to run and we wanted an example where we could make a quantitative comparison with SSA.

TABLE II. Sample standard deviations (for a sample size of  $n=10\,000$ ) for the final states in example 1 as computed by SSA, explicit-tau, the original implicit-tau, and the interlaced implicit-tau methods, with step sizes as described in the text.

	SSA	Explicit tau	Implicit tau	Interlaced implicit tau
Sample standard deviation: $x_1(0.2)$	18.42	24.76	3.07	17.74
Sample standard deviation: $x_2(0.2)$	10.49	13.45	5.34	10.24
Sample standard deviation: $x_3(0.2)$	3.91	3.88	3.89	3.91



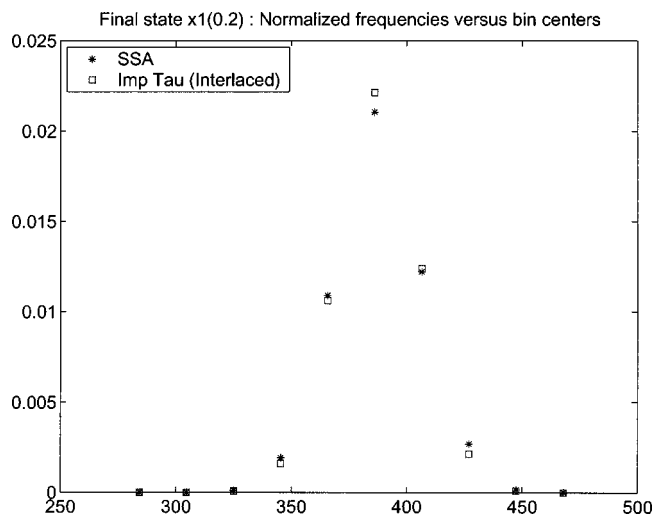


FIG. 10. Final state histogram for  $x_1$  in example 1, as computed by the SSA (stars), and the implicit-tau method (squares) with interlaced stepping.

## VI. CONCLUSIONS

We have shown how stiffness manifests itself in the simulation of chemical reactions at both the continuous, deterministic level and the discrete, stochastic level. While the explicit-tau method is an important first step in the efficient simulation of stochastic chemical systems, it must use a very small step size when applied to stiff systems.

We have proposed an implicit version of the tau-leaping method. We have demonstrated through numerical simulations that the implicit-tau method achieves the same level of accuracy as the explicit-tau method when the latter is stable, and that the new method overcomes the instability problem of explicit tau for larger step sizes. For large step sizes, we have seen that the implicit-tau method resolves well the slow stochastic components, and it captures the mean of the fast components. We have introduced a method for recovering the distributions of the fast stochastic components based on a time-stepping scheme that interlaces several small time steps with several large time steps.

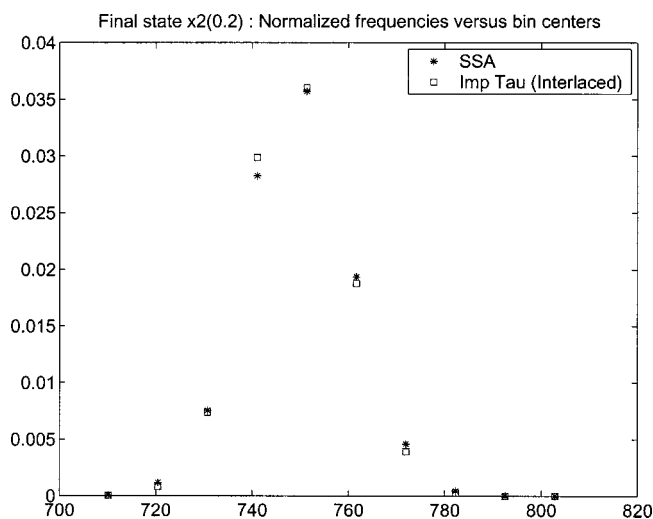


FIG. 11. Final state histogram for  $x_2$  in example 1, as computed by the SSA (stars), and the implicit-tau method (squares) with interlaced stepping.

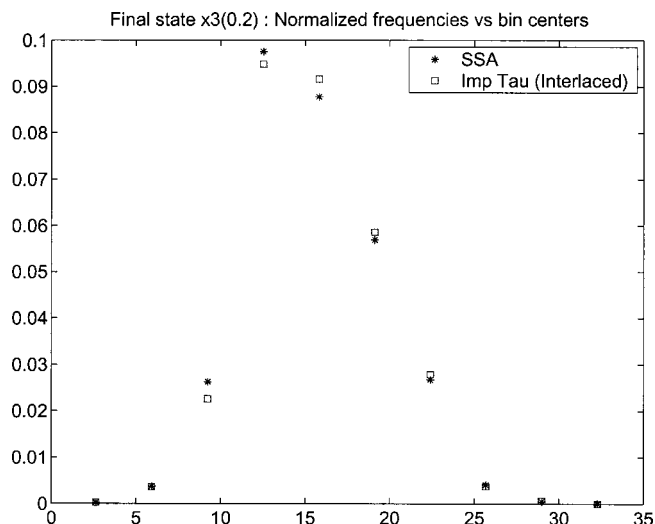


FIG. 12. Final state histogram for  $x_3$  in example 1, as computed by the SSA (stars), and the implicit-tau method (squares) with interlaced stepping.

## ACKNOWLEDGMENTS

We would like to thank John Doyle for bringing us together and for making us aware of the need for multiscale methods in the simulation of biochemical networks. We would also like to thank Andrew Hall for assisting us with the numerical experiments. This work was supported by the Air Force Office of Scientific Research and the California Institute of Technology under DARPA Award No. F30602-01-2-0558.

## APPENDIX: THE REVERSIBLE ISOMERIZATION REACTION

The pair of reactions  $S_1 \xrightleftharpoons[c_2]{c_1} S_2$  describes the reversible conversion of two isomeric species  $S_1$  and  $S_2$  into each other. The reaction probability rate constants  $c_j$  for these monomolecular channels are numerically equal to the rate constants  $k_j$  that appear in the corresponding deterministic reaction rate equations for the species concentrations.<sup>17</sup> The propensity functions and state-change vectors for these reaction channels are

$$a_1(\mathbf{x}) = c_1 x_1, \quad a_2(\mathbf{x}) = c_2 x_2, \quad (\text{A1})$$

$$\mathbf{v}_1 = (-1, +1), \quad \mathbf{v}_2 = (+1, -1). \quad (\text{A2})$$

In the absence of any other reaction channels, the total number of isomers  $x_T$  will remain constant in time. This circumstance allows us to eliminate one of the species variables, say the  $S_2$  variable, in favor of the other

$$X_2(t) = x_T - X_1(t), \quad (\text{A3})$$

and thereby obtain a mathematically simpler univariate problem. In this Appendix, we shall derive exact expressions for the mean and variance of  $X_1(t) \equiv X(t)$  for the initial condition  $X(t_0) = x_0$ , where  $x_0$  and  $x_T$  may be any two integers satisfying  $0 \leq x_0 \leq x_T$ . We should note that solutions to the full chemical master equation are known for the special cases  $x_0 = 0$  and  $x_0 = x_T$ .<sup>18</sup>

TABLE III. Sample means and standard deviations (for a sample size of  $n = 10\,000$ ) for the final state of  $x_2$  in example 2 as computed by ODE solver, SSA, explicit-tau, the original implicit-tau, and the interlaced implicit-tau methods, with step sizes as described in the text.

	ODE	SSA	Explicit tau	Implicit tau	Interlaced implicit tau
Sample mean: $x_2(0.01)$	95.12	95.10	95.07	95.07	95.05
Standard deviation: $x_2(0.01)$	NA	2.15	2.14	2.21	2.18

The process  $X(t)$  evolves according to the following dynamical rules: If  $X(t) = x$ , then in the next infinitesimal time  $dt$ ,  $X$  will increase by 1 or decrease by 1 with the respective probabilities  $W_+(x)dt$  and  $W_-(x)dt$ , where

$$W_+(x) = c_2(x_T - x), \quad W_-(x) = c_1x. \tag{A4}$$

This kind of dynamical behavior identifies  $X(t)$  as a birth-death-type Markov process with stepping probability rate functions  $W_+(x)$  and  $W_-(x)$ . Quite generally for such a process, the time derivatives of the mean and variance are given by<sup>19</sup>

$$\frac{d\langle X(t) \rangle}{dt} = \langle A(X(t)) \rangle, \tag{A5}$$

$$\begin{aligned} \frac{d \text{var}\{X(t)\}}{dt} &= 2(\langle X(t)A(X(t)) \rangle - \langle X(t) \rangle \langle A(X(t)) \rangle) \\ &+ \langle D(X(t)) \rangle, \end{aligned} \tag{A6}$$

where

$$A(x) \equiv W_+(x) - W_-(x), \quad D(x) \equiv W_+(x) + W_-(x). \tag{A7}$$

For the stepping functions (A4),  $A$  and  $D$  are easily calculated to be

$$A(x) = c_2x_T - (c_1 + c_2)x,$$

$$D(x) = c_2x_T + (c_1 - c_2)x.$$

When these forms are substituted into Eqs. (A5) and (A6), we obtain

$$\frac{d\langle X(t) \rangle}{dt} = c_2x_T - (c_1 + c_2)\langle X(t) \rangle, \tag{A8}$$

$$\begin{aligned} \frac{d \text{var}\{X(t)\}}{dt} &= -2(c_1 + c_2)\text{var}\{X(t)\} \\ &+ c_2x_T + (c_1 - c_2)\langle X(t) \rangle. \end{aligned} \tag{A9}$$

The time-evolution equation (A8) for the mean  $\langle X(t) \rangle$  is mathematically identical to the associated deterministic reaction rate equation, although expressed here in terms of the molecular populations instead of concentrations. This is not so in general, but it is the case whenever the propensity functions are linear in the species variables. Equation (A8) has the form of the first-order linear differential equation  $dy(t)/dt = ky(t) + f(t)$ , for which the general solution in quadrature form is

$$y(t) = e^{k(t-t_0)} \left\{ y(t_0) + \int_{t_0}^t f(t') e^{-k(t'-t_0)} dt' \right\}, \tag{A10}$$

as may readily be verified by direct differentiation. Evaluating this quadrature form for Eq. (A8) using the initial condition  $\langle X(t_0) \rangle = x_0$  gives

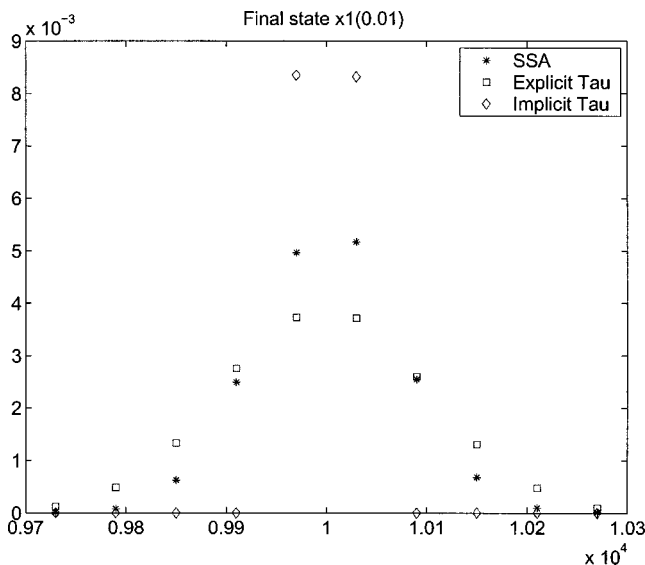


FIG. 13. Final state histogram for  $x_1$  in example 2, as computed by the SSA (stars), the explicit-tau method with step size  $5 \times 10^{-6}$  (squares), and the implicit-tau method with step size  $5 \times 10^{-3}$  (diamonds). Note that most of the variation (as computed by SSA) is within 1% deviation from the mean value of  $10^4$ , and thus the noise in this variable may be regarded as negligible. The plot of the histogram has been scaled to fit the narrow range of values of  $x_1$ .

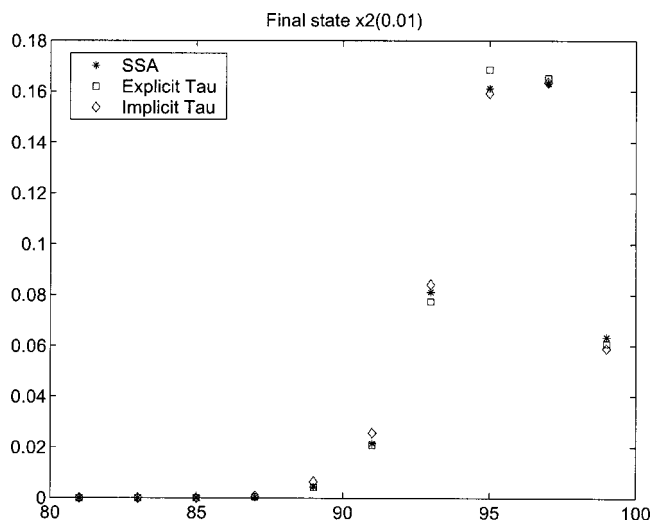


FIG. 14. Final state histogram for  $x_2$  in example 2, as computed by the SSA (stars), the explicit-tau method with step size  $5 \times 10^{-6}$  (squares), and the implicit-tau method with step size  $5 \times 10^{-3}$  (diamonds). In contrast to the fluctuations in  $x_1$ , the fluctuations in this variable are not negligible.

$$\langle X(t) \rangle = x_0 + (x_\infty - x_0)(1 - e^{-(c_1 + c_2)(t-t_0)}), \quad (\text{A11})$$

where

$$x_\infty \equiv \frac{c_2 x_T}{c_1 + c_2}. \quad (\text{A12})$$

By substituting the result (A11) into Eq. (A9), we obtain for the variance a differential equation that is once again of the first-order linear form. When we evaluate the corresponding quadrature solution (A10) using the initial condition  $\text{var}\{X(t_0)\} = 0$ , we get

$$\begin{aligned} \text{var}\{X(t)\} = & \frac{c_1 x_\infty}{(c_1 + c_2)} (1 - e^{-2(c_1 + c_2)(t-t_0)}) \\ & + \left( \frac{(c_1 - c_2)(x_0 - x_\infty)}{(c_1 + c_2)} \right) (e^{-(c_1 + c_2)(t-t_0)} \\ & - e^{-2(c_1 + c_2)(t-t_0)}). \end{aligned} \quad (\text{A13})$$

We note in passing that Eqs. (A11) and (A13) imply the asymptotic results

$$\langle X(\infty) \rangle = x_\infty \quad \text{and} \quad \text{var}\{X(\infty)\} = \frac{c_1 x_\infty}{(c_1 + c_2)}. \quad (\text{A14})$$

<sup>1</sup>H. H. McAdams and A. Arkin, *Trends Genet.* **15**, 65 (1999).

<sup>2</sup>H. H. McAdams and A. Arkin, *Proc. Natl. Acad. Sci. U.S.A.* **94**, 814 (1997).

<sup>3</sup>A. Arkin, J. Ross, and H. H. McAdams, *Genetics* **149**, 1633 (1998).

<sup>4</sup>N. Fedoroff and W. Fontana, *Science* **297**, 1129 (2002).

<sup>5</sup>M. A. Gibson and J. Bruck, *J. Phys. Chem.* **104**, 1876 (2000).

<sup>6</sup>D. T. Gillespie, *J. Chem. Phys.* **115**, 1716 (2001).

<sup>7</sup>As here defined,  $\nu_{ij}$  is the  $\nu_{ji}$  of Refs. 6, 10, 11. The present indexing corresponds to the commonly accepted definition of the *stoichiometric matrix*.

<sup>8</sup>The Poisson random variable  $\mathcal{P}(a, \tau)$  is the integer-valued random vari-

able defined by

$$\text{Prob}\{\mathcal{P}(a, \tau) = n\} = [e^{-a\tau}(a\tau)^n]/n! \quad (n = 0, 1, \dots).$$

Both the mean and the variance of  $\mathcal{P}(a, \tau)$  are equal to  $a\tau$ .  $\mathcal{P}(a, \tau)$  can be interpreted physically as the number of events that will occur in any finite time  $\tau$ , given that the probability of an event occurring in any future infinitesimal time  $dt$  is  $adt$ .

<sup>9</sup>We denote by  $\mathcal{N}(m, \sigma^2)$  the normal (or Gaussian) random variable with mean  $m$  and variance  $\sigma^2$ . This random variable has the useful property that  $\mathcal{N}(m, \sigma^2) = m + \sigma\mathcal{N}(0, 1)$ .

<sup>10</sup>D. T. Gillespie, *J. Chem. Phys.* **113**, 297 (2000).

<sup>11</sup>D. T. Gillespie, *J. Phys. Chem. A* **106**, 5063 (2002).

<sup>12</sup>P. F. Kloeden and E. Platen, *Numerical Solution of Stochastic Differential Equations*, 2nd ed. (Springer, Berlin, 1995).

<sup>13</sup>P. M. Burrage and K. Burrage, A variable stepsize implementation for stochastic differential equations, *SIAM J. Sci. Comput. (USA)* **24**, 848 (2002).

<sup>14</sup>In the *thermodynamic limit*, the species populations  $x_i$  and the system volume  $\Omega$  diverge *together*, and *proportionately*. It turns out that, in this limit, all propensity functions  $a_j(\mathbf{x})$  diverge *linearly* with the system size, because the propensity function for an  $m$ th-order reaction will contain  $m$  factors  $x_i$  along with a factor  $\Omega^{-(m-1)}$ . As a consequence, while the terms under the first summation sign in Eq. (4) are roughly proportional to the system size, the terms under the second summation sign are roughly proportional to the *square root* of the system size. So, in the thermodynamic limit, the latter terms typically become negligibly small compared to the former terms. Of course, real systems, no matter how large, are necessarily *finite*, and in situations where the terms in the first summation in Eq. (4) add up to practically zero (for instance at equilibrium), the fluctuating second sum can become important.

<sup>15</sup>U. M. Ascher and L. R. Petzold, *Computer Methods for Ordinary Differential Equations and Differential-Algebraic Equations* (SIAM, 1998).

<sup>16</sup>D. T. Gillespie, *Markov Processes: An Introduction for Physical Scientists* (Academic, Philadelphia, PA, 1992).

<sup>17</sup>D. T. Gillespie, *J. Comput. Phys.* **22**, 403 (1976).

<sup>18</sup>I. G. Curtiss and P. J. Staff, *J. Chem. Phys.* **44**, 990 (1976).

<sup>19</sup>See Ref. 16, p. 385, Eqs. (6.1-29) and (6.1-30), and note that the functions  $v(x)$  and  $a(x)$  appearing in those equations are defined in Eqs. (6.1-13) to be the same as our functions  $A(x)$  and  $D(x)$ , respectively.